Journal of Applied Mechanics and Technical Physics, Vol. 45, No. 1, pp. 37–44, 2004

TOPOGRAPHY AND DISPERSION EFFECTS IN BOTTOM LAYER DYNAMICS

K. N. Gavrilova

UDC 532.59

A hyperbolic model of a shallow water flow is considered with allowance for nonlinear and dispersion effects. The structure of traveling waves above a flat bottom is studied. Stability of small disturbances of a homogeneous flow and development of instability of a nonstationary flow above an inclined bottom are analyzed.

Key words: *shallow water equations, roll wave, homogeneous liquid, hyperbolic model with dispersion.*

Introduction. Under certain angles of inclination, a homogeneous flow in long channels becomes unstable, which results in the development of waves that were called roll waves.

The mathematical theory of roll waves was first constructed by Dressler [1]. For turbulent flows, where the force of gravity is balanced by the force of friction on the channel bottom, it was found that the class of traveling waves for shallow water equations with turbulent friction contains periodic discontinuous solutions, and there are no continuous periodic solutions. The critical values of the Froude number for shallow water equations with turbulent friction (constant friction coefficient) is $\mathrm{Fr} = 2$, as was shown in [2, 3].

The dependence of the growth rate of disturbances on the wave length was analyzed in [4]. It was shown that linear waves with the maximum growth rate correspond to the developed stage of experimentally observed roll waves [5].

Introduction of dissipative terms into the shallow water equations made it possible to prove the existence of a smooth periodic solution [6]. It was shown [7, 8] that smooth periodic low-amplitude solutions in the dissipative model are unstable, and finite-amplitude roll waves arise in the course of flow evolution; the structure of these waves is similar to periodic waves constructed by Dressler.

A model taking into account the influence of dispersion on wave evolution is considered in the present work. The model is hyperbolic and adequately approximates the second approximation of the shallow water theory. The structure of traveling waves above a flat bottom is studied. The results calculated for the nonstationary problem of wave generation by an obstacle moving on the flat bottom are compared with the results obtained for the Boussinesq model [9].

In the case of an inclined bottom, stability of small disturbances of a homogeneous flow is analyzed with allowance for friction, and the critical Froude number, which determines the transition from stable to unstable flow, is found. The dynamics of roll waves in an inclined channel is numerically studied as a nonlinear stage of evolution of homogeneous flow instability, and the influence of dispersion on the structure of roll waves is determined.

1. Analysis of a Hyperbolic Model. 1.1. *Formulation of the Problem.* We consider the evolution of a thin layer of a heavy liquid located under a quiescent layer of another lighter immiscible liquid. The one-layer shallow water equations describe the structure of the submerged layer if the thickness of the upper quiescent layer is much greater than the thickness of the lower layer of the heavier liquid. The equations of motion, instead of the acceleration of gravity g, involve the reduced acceleration $g^* = (\rho^- - \rho^+)g/\rho^-$, where ρ^+ and ρ^- are the densities of the upper and lower layers, respectively.

In hydraulics, the dependence of velocity on the coordinate y normal to the bottom is eliminated by averaging; therefore, $u = u(t, x)$, and acceleration along the y axis is neglected. The latter means that the pressure distribution

Lavrent'ev Institute of Hydrodynamics, Siberian Division, Russian Academy of Sciences, Novosibirsk 630090.
Translated from Prikladnaya Mekhanika i Tekhnicheskaya Fizika, Vol. 45, No. 1, pp. 46–55, January–February, 2004. Original article submitted March 14, 2003; revision submitted April 22, 2003.

0021-8944/04/4501-0037

is hydrostatic [2] and equations are derived for the layer thickness $h(t,x)$ and depth-averaged velocity $u(t,x)$. It is impossible to describe the structure of wave fronts within the framework of the classical shallow water theory. It is known that a wave train appears behind the front when disturbances propagate over a quiescent liquid. The wave length is comparable to the homogeneous layer thickness, i.e., an undular bore arises; nonhydrostatisity of the pressure distribution on the wave front is largely responsible for undular bore formation. The undular bore is modeled by various variants of the Boussinesq and Korteweg–de Vries equations [2], where the dispersion effects are described by terms containing higher-order derivatives. The corresponding models are not described by systems of hyperbolic equations. As an example, we can cite the nonstationary variant of Serre's model [10]

$$h_t + (uh)_x = 0, \qquad u_t + \Big(\frac{1}{2}\,u^2 + g^* h + æh\,\frac{d^2h}{dt^2}\Big)_x = 0, \tag{1}$$

where æ is the ratio of the vertical and horizontal scales. This parameter can be brought to an arbitrary constant by appropriate extension of variables.

The hyperbolic model with dispersion was considered in [11]. To allow for nonhydrostatisity of the pressure distribution in the liquid layer, the averaged equations involve the quantity p^*, which is the pressure deficit on the channel bottom:

$$h_t + (hu)_x = 0, \qquad u_t + uu_x + g^* h_x + p^*_x = 0. \tag{2}$$

Along with the averaged quantities [layer thickness $h(t,x)$ and velocity $u(t,x)$], Eq. (2) involves variables that characterize the flow at a given point. In equilibrium, the mean and instantaneous values are identical. Let $\eta(t,x)$ be the depth and $v(t,x)$ be the vertical velocity of the liquid on the surface. The difference between the mean depth $h(t,x)$ and instantaneous depth $\eta(t,x)$ appears when a wave whose length is comparable to the longitudinal spatial scale used to obtain the mean value of $h(t,x)$ starts propagating over the liquid in the neighborhood of the point x.

The difference between $h(t,x)$ and $\eta(t,x)$ is assumed to be small: $|\eta/h - 1| \ll 1$. The equations for $\eta(t,x)$ and $v(t,x)$ have the form [11]

$$\eta_t + u\eta_x = v, \qquad h(v_t + uv_x) = \beta p^*, \tag{3}$$

where β is the ratio of the vertical and horizontal scales in passing to the long-wave approximation. This parameter can be made equal to unity by appropriate extension of variables. The first equation in (3) is the kinematic condition on the liquid surface, and the second one is obtained by integration of the momentum equation for the vertical component of velocity over the entire layer with allowance for no-slip conditions on the bottom and by virtue of the linear distribution of the vertical component of velocity over the depth.

To close system (2), (3), it is sufficient to express p^* through the sought variables, e.g., through h and η: $p^* = p^*(h,\eta)$. Since $|h - \eta| \ll h$, then, with allowance for the equilibrium condition $p^*(h,h) \equiv 0$, the expression for p^* can be chosen in the following form:

$$p^* = \alpha g^* (h - \eta). \tag{4}$$

For $\alpha \to 0$, Eqs. (2) are independent of system (3) and transform to the classical shallow-water equations. For $\alpha \to \infty$, the system obtained is equivalent to system (1), since $h \equiv \eta$. For finite values of the parameter α, system (2)–(4), being intermediate between the first and second shallow water approximation, describes the dispersion properties and remains hyperbolic. It was shown [11] that system (2)–(4) is hyperbolic.

System (2)–(4) can be modified to describe waves above an inclined bottom. In this case, it takes the form

$$\begin{gathered} h_t + (hu)_x = 0, \qquad u_t + (u^2/2 + bh + b\alpha(h - \eta))_x = b\tan\varphi - c_{\mathrm{f}} u^2/h, \\ \eta_t + u\eta_x = v, \qquad h(v_t + uv_x) = \beta\alpha b(h - \eta), \end{gathered} \tag{5}$$

where φ is the channel slope, c_{f} is the friction coefficient, and $b = g^* \cos\varphi$.

For $c_{\mathrm{f}} = 0$ and $\varphi = 0$, the solution of system (5) is the traveling waves above a flat bottom. If we introduce the function $z(x)$, which defines the type of the local obstacle, into the second equation of the system, the model becomes applicable for description of waves generated by an obstacle moving over the bottom [11].

For an inclined plane, the solution of system (5) is a stationary flow ($v = 0$, $\eta = h_0$, $h = h_0$, and $u = u_0$); in this case, we have $h_0 = c_{\mathrm{f}} u_0^2/(g^* \sin\varphi)$.

In the dimensionless variables

$$\bar h = h/h_0, \qquad \bar u = u/\sqrt{g^* h_0 \cos\varphi}, \qquad \bar\eta = \eta/h_0,$$

$$\bar x = x/h_0, \qquad \bar t = t\sqrt{g^* \cos\varphi/h_0}, \qquad \bar v = v/\sqrt{g^* h_0 \cos\varphi},$$

system (5) takes the form (the bar is omitted)

$$\begin{gathered} h_t + (hu)_x = 0, \qquad u_t + (u^2/2 + h + \alpha(h-\eta))_x = c_{\mathrm f}(\gamma - u^2/h), \\ \eta_t + u\eta_x = v, \qquad h(v_t + uv_x) = \beta\alpha(h-\eta), \end{gathered} \tag{6}$$

where $\gamma = \tan\varphi/c_{\mathrm f}$. If a homogeneous flow with a depth h_0 is formed, the Froude number of such a flow is determined by the parameter γ: $\mathrm{Fr}^2 = u_0^2/h_0 = \gamma$.

1.2. *Analysis of Small Disturbances.* Linearization of system (6) on the solution $h = 1$, $u = \sqrt{\gamma}$, $\eta = 1$, $v = 0$ yields the following equations for disturbances:

$$\begin{gathered} h_t + \sqrt{\gamma} h_x + u_x = 0, \qquad u_t + (1+\alpha)h_x + \sqrt{\gamma}u_x - \alpha\eta_x + c_{\mathrm f}(2\sqrt{\gamma}u - \gamma h) = 0, \\ \eta_t + \sqrt{\gamma}\eta_x - v = 0, \qquad v_t + \sqrt{\gamma}v_x - \beta\alpha(h-\eta) = 0. \end{gathered} \tag{7}$$

Substituting the solution $U = \hat U \exp\left(i(\sigma\hat x - \omega\hat t)\right)$, where $U = (h, u/\sqrt{\gamma}, \eta, v/\sqrt{\gamma})^{\mathrm t}$, $\hat U = (\hat h, \hat u, \hat\eta, \hat v)^{\mathrm t}$, $\hat x = c_{\mathrm f}\gamma x$; $\hat t = c_{\mathrm f}\sqrt{\gamma^3}t$, into Eq. (7), we obtain the algebraic relations

$$(\sigma-\omega)\hat h + \sigma\hat u = 0, \qquad ((1+\alpha)i\sigma - 1)\hat h + (2 + i\gamma(\sigma-\omega))\hat u - i\alpha\sigma\hat\eta = 0,$$

$$i\gamma(\sigma-\omega)\hat\eta - \hat v/c_{\mathrm f} = 0, \qquad (\beta\alpha/c_{\mathrm f})\hat h - (\beta\alpha/c_{\mathrm f})\hat\eta - i\gamma^2(\sigma-\omega)\hat v = 0$$

and, after simple transformations, the dispersion relation

$$i\gamma^4 q^4 + 2\gamma^3 q^3 - \Big(\gamma^3\sigma((1+\alpha)i\sigma - 1) + \frac{\beta\alpha i\gamma}{c_{\mathrm f}^2}\Big)q^2 - \frac{2\beta\alpha}{c_{\mathrm f}^2}\,q + \frac{\beta\alpha}{c_{\mathrm f}^2}\,\sigma(i\sigma - 1) = 0 \tag{8}$$

($q = \sigma - \omega$).

The solution is stable for $\operatorname{Im}\omega < 0$, i.e., $\operatorname{Im} q > 0$. For $\alpha = 0$, Eq. (8) yields the known condition of stability $\gamma < 4$ for shallow water equations with friction [4]. A numerical study of the dependence $\omega = \omega(\sigma)$ for $c_{\mathrm f} = 1$ and $\beta = 2$ with the parameter α varied within a wide range ($1 < \alpha < 75$) shows that the critical value γ_{cr} changes insignificantly (γ_{cr} is located in the ε-neighborhood of the point $\gamma = 4$, where $\varepsilon = 0.1$). Thus, the change in the parameter α responsible for wave dispersion in the system has a weak effect on stability boundaries.

1.3. *Comparison of the Properties of the Second Approximation of the Shallow Water Theory with the Hyperbolic Model.* We study two systems of equations for the liquid flow above a flat bottom: the hyperbolic system (5) ($\alpha < \infty$, $c_{\mathrm f} = 0$, and $\varphi = 0$)

$$h_t + (uh)_x = 0, \qquad u_t + (u^2/2 + g^* h + g^*\alpha(h-\eta))_x = 0,$$

$$\eta_t + u\eta_x = v, \qquad h(v_t + uv_x) = g^*\beta\alpha(h-\eta)$$

and system (1), which is one variant of the Boussinesq equation.

We consider the second approximation of the shallow water equations (1). Let the solutions depend only on the variable $\xi = x - Dt$. The traveling waves of system (1) were found in [10]:

$$h(u-D) = -h_0 D,$$

$$u^2/2 - Du + g^* h + æ(D^2 hh'' - 2Duhh'' + u^2 hh'' - Dhu'h' + huh'u') = g^* h_0$$

(the prime denotes differentiation with respect to the variable ξ). The traveling wave profile is expressed in quadratures as

$$\xi = \xi_0 \pm \int_{h_0}^{h} \frac{Dh_0\,ds}{s\sqrt{2F_\infty(s)}}, \tag{9}$$

where

$$F_\infty(h) = (-g^*(h-h_0) + (D^2/2 + g^* h_0)\ln(h/h_0) + D^2(h_0^2/h^2 - 1)/4)/æ.$$

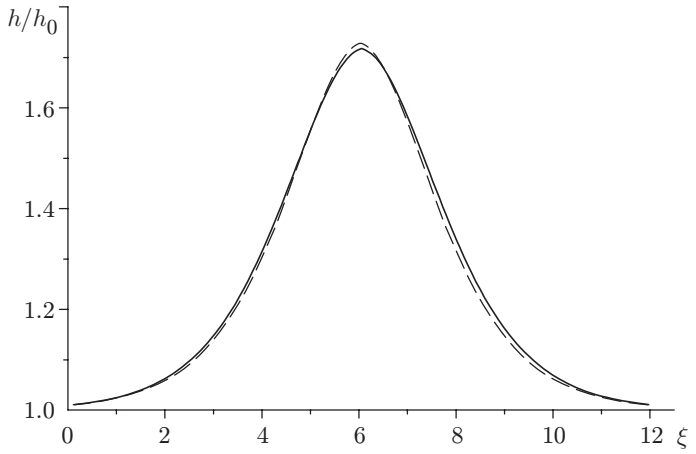

Fig. 1. Profiles of solitons ($D = 1.3$): the solid and dashed curves show the calculations by the hyperbolic system (5) and Boussinesq equations (1), respectively.

If the equilibrium state is chosen as h_0, it follows from (9) that the necessary condition for solution existence is the positiveness of the function $F_\infty(h)$ in the neighborhood of the point $h = h_0$. Since $F_\infty(h_0) = 0$ and $F'_\infty(h_0) = 0$, the inequality $F''_\infty(h_0) > 0$, which ensures the positiveness of the function $F_\infty(h)$ near the point h_0, is satisfied if and only if

$$\sqrt{g^* h_0} < D. \tag{10}$$

The wave profile for the velocity D satisfying inequality (10) is shown by the dashed curve in Fig. 1.

Let us now consider the hyperbolic system. The traveling waves are described by the following equations:

$$(h(u - D))' = 0, \qquad (u^2/2 - Du + (1 + \alpha)g^* h - g^* \alpha \eta)' = 0,$$

$$(u - D)\eta' = v, \qquad h(u - D)v' = g^* \beta \alpha (h - \eta).$$

For this system, the profile of the traveling wave is expressed in quadratures [11]

$$\xi = \xi_0 \pm \int_{h_0}^{h} \frac{D h_0 a(s)\, ds}{s\sqrt{2F_\alpha(s)}},$$

where $a(h) = 1 - (D^2 h_0^2/(g^* h^3) - 1)/\alpha$ and

$$F_\alpha(h) = \frac{\beta}{2}\Big(- 2g^* \Big(1 + \frac{1}{\alpha}\Big)(h - h_0) + \frac{D^2 h_0^2}{2\alpha}(\alpha - 1)\Big(\frac{1}{h^2} - \frac{1}{h_0^2}\Big)$$

$$+ \Big(1 + \frac{1}{\alpha}\Big)(D^2 + 2g^* h_0) \ln\Big(\frac{h}{h_0}\Big) + \frac{D^2 h_0^2}{3\alpha}\Big(2h_0 + \frac{D^2}{g^*}\Big)\Big(\frac{1}{h^3} - \frac{1}{h_0^3}\Big) - \frac{D^4 h_0^4}{5g^* \alpha}\Big(\frac{1}{h^5} - \frac{1}{h_0^5}\Big)\Big).$$

The inequality that ensures positiveness of the function $F_\alpha(h)$ in the neighborhood of the point h_0 is satisfied if and only if

$$\sqrt{g^* h_0} < D < \sqrt{(1 + \alpha)g^* h_0}. \tag{11}$$

The wave profile for the velocity D satisfying inequality (11) is shown by the solid curve in Fig. 1. Numerical calculation of integrals by the fourth-order Runge–Kutta method for $h_0 = 1$, $g^* = 1$, $\alpha = 8$, $\beta = 2$, $æ = 1/2$, and $D = 1.3$ demonstrated the effectiveness of approximation of the model of the second approximation of the shallow water theory by the hyperbolic model. The error in using model (1) instead of model (5) for constructing solitons is rather low already for $\alpha \approx 1$ and rapidly decreases as $\alpha \to \infty$. A comparison of nonstationary solutions in the case of hyperbolic approximation of the second approximation of the shallow water equations is given below.

1.4. *Generation of Nonstationary Waves in the Flow Above a Local Obstacle.* To verify the effectiveness of approximation of the Boussinesq equations by hyperbolic models, we consider the generalized Boussinesq model. The system studied in [9] has the following form in the notation used in the present work:

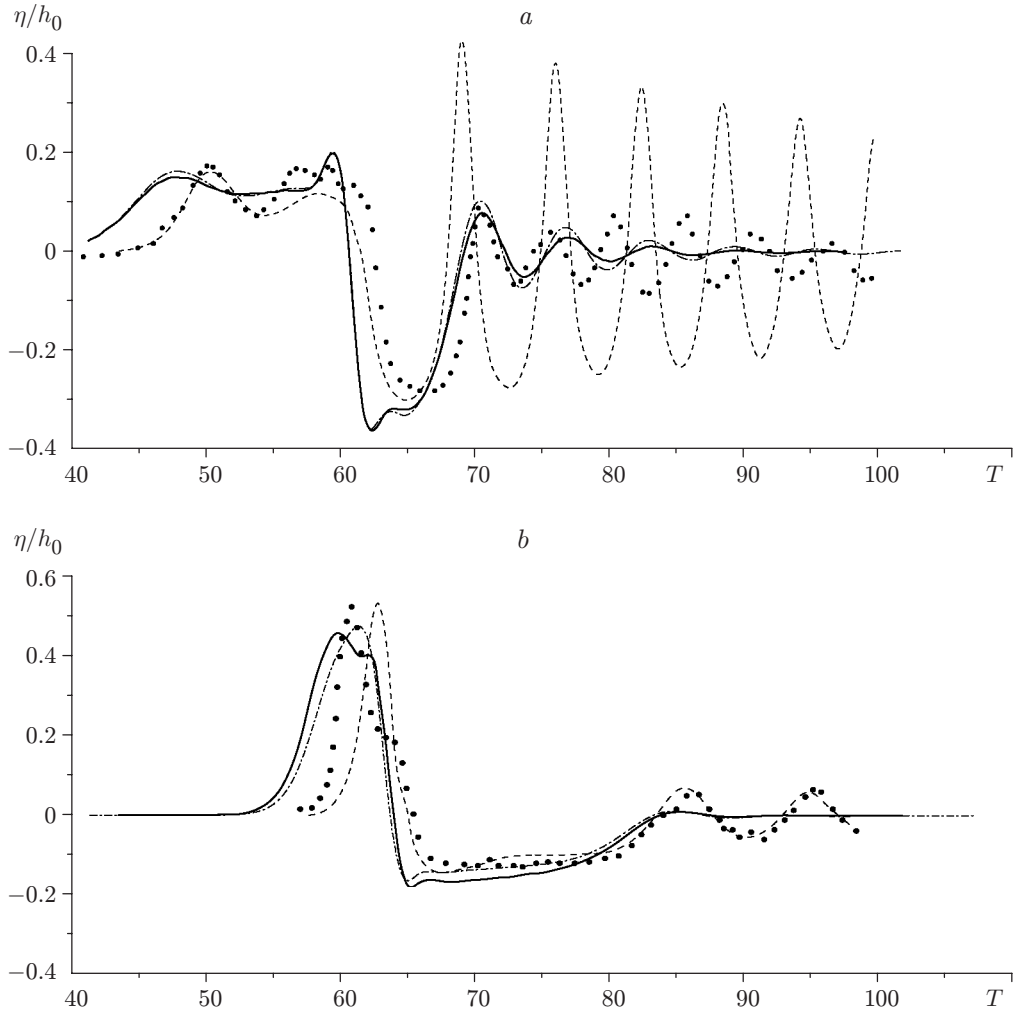

Fig. 2. Experimental and calculated depths of the liquid layer η versus time T: Fr = 0.82 (a) and 1.12 (b); the points show the experimental data of [9]; the calculation results obtained by models (13), (6), and (12) are plotted by the solid, dot-and-dashed, and dashed curves, respectively.

$$h_t + (uh)_x = 0, \qquad u_t + (u^2/2 + h + z - u_{xt}/3)_x = 0. \tag{12}$$

The function $z(x)$ defines the shape of the local obstacle.

As for model (5), hyperbolic approximation of system (12) can be represented in the form

$$h_t + (uh)_x = 0, \qquad u_t + (u^2/2 + h + z + \beta\alpha(h-\eta)/3)_x = 0,$$
$$\eta_t = v, \qquad v_t = \beta\alpha(h-\eta). \tag{13}$$

System (13) was used to solve the nonstationary problem of wave generation by a local obstacle. The results are compared below with experimental and numerical data for model (12) taken from [9].

Note, Eqs. (12) do not admit Galileo's transform. Therefore, in addition to (13), we used the invariant model (6) ($c_{\mathrm{f}} = 0$ and $\varphi = 0$) with a function defining the obstacle shape as hyperbolic approximation.

System (13) was numerically solved by the Godunov method based on the problem of decay of an arbitrary discontinuity with allowance for the multiple contact characteristic $x \equiv \mathrm{const}$.

The motion of the obstacle with a constant velocity D started from the state at rest ($h \equiv h_0$ and $u = 0$). The calculation was performed for various values of the Froude number $\mathrm{Fr} = D/\sqrt{bh_0} = 0.82$–$1.12$. The obstacle was a cylindrical segment of height $z_m/h_0 = 0.2$ with a base width $L/h_0 = 1.23$. The results obtained were compared with the calculation results by model (12) [9] and experimental data [9].

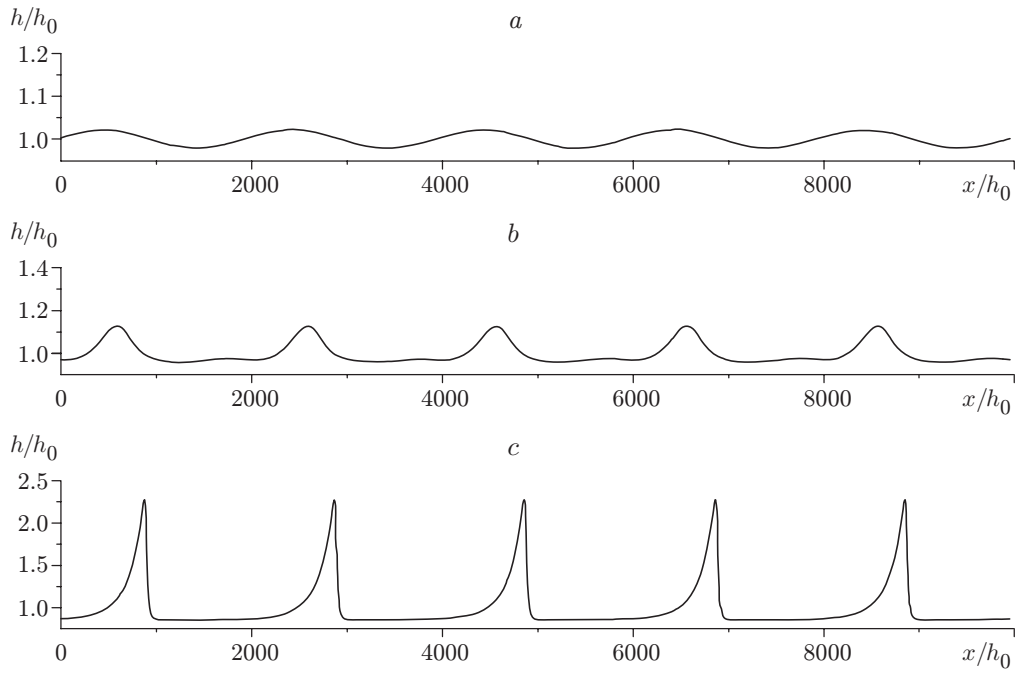

Fig. 3. Evolution of periodic waves [calculation by model (6)]: $t = 0$ (a), 12.72 (b), and 70.71 (c).

The main features of the waves noted in [9], namely, generation of an upstream-advancing solitary wave, an elongating depressed region, and a trailing wave train on the leeward side of the obstacle, were also observed in the numerical solution.

Figure 2 shows the experimental data of [9] and also the numerical results calculated by model (12), by hyperbolic model (13) for $\alpha = 1$ and $\beta = 3$, and by model (6). The calculations were performed for high subcritical and low supercritical speeds. The results calculated by the hyperbolic model for high subcritical speeds ($0.8 < \mathrm{Fr} < 0.9$) are in good agreement with the data calculated by model (12) and experimental values of the amplitude. For the trailing wave train, the calculated amplitude is lower than the experimental one (the waves decay). Model (13) does not yield weakly decaying oscillations on the leeward side of the obstacle, which appear in model (12).

For low supercritical speeds ($1.1 < \mathrm{Fr} < 1.2$), the hyperbolic model predicts the same maximum values of the amplitude and the same depressed region as the model of [9]. The results of numerical calculations by the hyperbolic models (13) and (6) are in agreement with experimental data and calculation results by model (12) for all parts of the wave profile except for the trailing wave train.

A comparison shows that a rather simple hyperbolic model adequately reflects all specific features of generation of nonstationary waves. The calculations by the hyperbolic model require much less time than the calculations by the predictor–corrector scheme and with the use of conversion of a triangular matrix for nonhyperbolic models [9].

2. Numerical Calculation of Nonstationary Flows on an Inclined Plane. It is known from experiments and natural observations that a homogeneous flow in an open channel with a constant angle of inclination is not always stationary. The homogeneous flow transforms into a wave flow in rather long channels with the angle of inclination greater than the critical value. Small waves are formed at a certain distance from the channel entrance. The amplitudes of disturbances are not high at the initial sector of the flow, and the liquid surface is smooth. Propagating downstream, however, the waves increase up to formation of developed bores. The flow at a large distance from the channel entrance is close to periodic and consists of bores and subsequent smooth regions. Such waves were called roll waves. A similar phenomenon is observed in gravity flows above an inclined bottom [12].

The experiments of [12] revealed the development of disturbances at the interface of two liquids with different densities in the case of a rather steep slope of the bottom providing supercritical motion of the lower layer. The wave disturbances move along the inclined plane with a velocity slightly higher than the mean flow velocity. They increase in amplitude and, finally, collapse, entraining the ambient liquid into the lower layer and generating an intense vortex flow near the interface. The evolution of the wave process in the two-layer system reminds generation

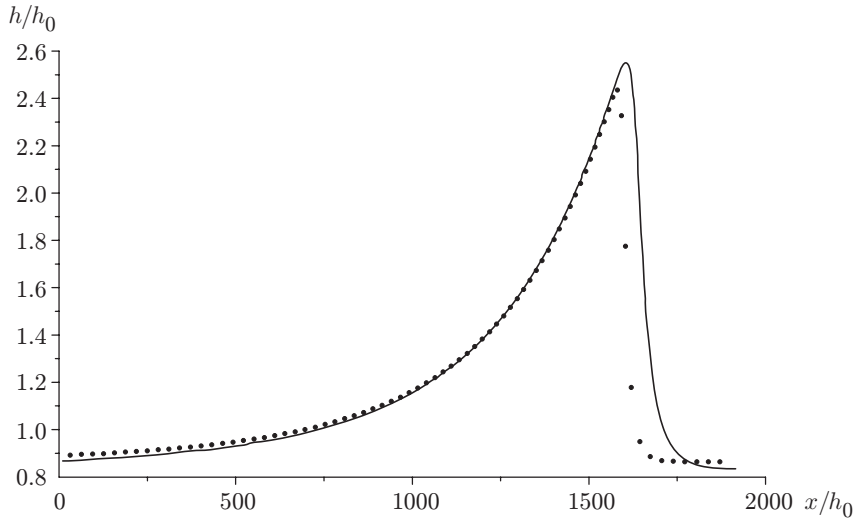

Fig. 4. Wave profiles calculated by model (6): the points and the curve refer to $\alpha = 0$ and 35, respectively.

of roll waves in supercritical flows in open channels, but the process of entrainment of the liquid from the upper layer can significantly affect the final stage of formation of a quasi-periodic flow. This effect is ignored in the present paper, and two-layer flows are simulated by the same equations as one-layer flows; the acceleration of gravity is replaced by the reduced acceleration g^*. In analyzing instability in two-layer flows, one can use the criterion derived in Sec. 1.2 for the hyperbolic model with dispersion (5).

The results of numerical calculations by model (6) for $\alpha = 1$, $\beta = 2$, and Fr = 3 (i.e., for Froude numbers higher than the critical value) are plotted in Fig. 3, which shows the evolution of disturbances in an inclined channel up to formation of developed roll waves. System (6) was numerically solved by the Godunov method based on the problem of decay of an arbitrary discontinuity with allowance for the multiple contact characteristic $dx/dt = u$.

In setting the initial periodic sinusoidal disturbances of an unstable homogeneous flow with the Froude number $\mathrm{Fr} = u_0/\sqrt{g^* h_0} = 3$ of the form $h_0(1 + \varepsilon_n \sin(\omega x))$ ($\varepsilon_n \approx 10^{-2}$), such that the computational domain contains a sufficient number of periods (five periods in Fig. 3), wave evolution rapidly reaches the nonlinear stage. The periodic disturbance for $t = 0$ is shown in Fig. 3a. At the initial stage of wave development, the amplitudes increase, but the wave profiles remain smooth though they lose symmetry (Fig. 3b). In further development, the amplitudes continue to increase, the wave profiles become steeper, and regions of the drastic increase in height (bores) are formed. In the classical shallow water equations ($\alpha = 0$), the bore is modeled by a moving discontinuity. For high values of the dispersion parameter α, the bore becomes more smooth. At large times, the growth of amplitudes is terminated, and a quasi-periodic regime is established. The roll waves consist of smooth regions separated by bores (Fig. 3c).

Figure 4 shows the profile of a developed wave for Fr = 3 and $\beta = 2$ for different values of the dispersion parameter. For $\alpha = 0$, the leading front of the wave is a discontinuity whose width tends to zero as the number of computational points increases. With increasing parameter α, the leading front of the wave becomes smooth. The smooth region of the wave changes little in a wide range of parameters.

Figure 5 shows the results of numerical simulation by model (6) of the evolution of a packet of roll waves developed from small disturbances of a homogeneous flow at the left boundary of the channel (Fr = 5, $\alpha = 1$, and $\beta = 2$). The evolution of roll waves is terminated at a certain distance from the channel entrance (on the left), and a flow close to periodic is formed. The effect of the dispersion parameter α on the structure of roll waves is manifested in a comparatively narrow region (in the region of the drastic increase in height); hence, the wave pattern is qualitatively similar to the case $\alpha = 0$ (cf. [11, Fig. 3.4]).

Conclusions. The model considered is applicable for a number of problems. In the case of a flat bottom, it confirms the validity of hyperbolic approximation in modeling leading fronts of disturbances and contains a solution that describes propagation of solitons in the range of velocities $\sqrt{bh_0} < D < \sqrt{(1+\alpha)bh_0}$ in a quiescent liquid of depth h_0. The model is applicable for the description of waves generated by a local obstacle moving over the bottom. The resultant phase pattern of waves (upstream-advancing solitary wave, elongating depressed region,

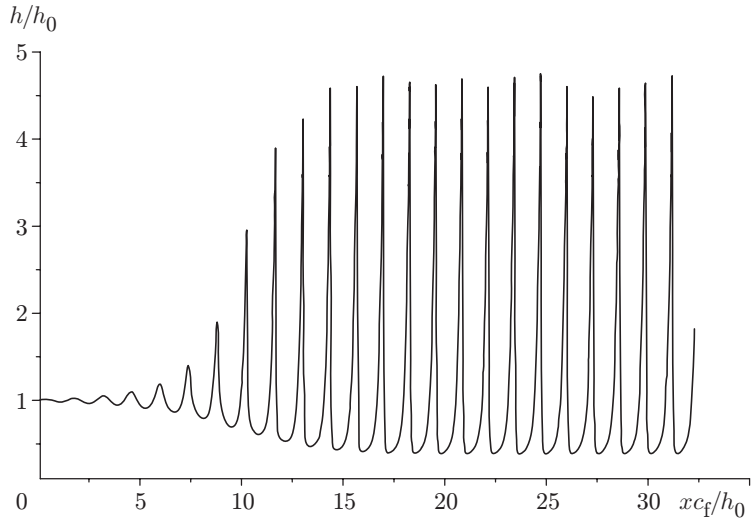

Fig. 5. Evolution of roll waves [calculation by model (6)].

and trailing wave train on the leeward side of the obstacle) agrees with experimental data and calculations by nonhyperbolic models [9]. In a numerical analysis of instability evolution in a nonstationary flow on an inclined bottom, the hyperbolic model predicts a regime close to periodic. The role of the dispersion parameter α is studied: this parameter ensures the velocity of disturbances higher than the wave velocity. For rather high values of α, the leading front of the wave becomes smooth. The model proposed combines effective approximation and calculation efficiency because it involves an explicit scheme including only the neighboring points.

This work was supported by INTAS (Grant No. 01-460).

REFERENCES

1. R. F. Dressler, "Mathematical solution of the problem of roll waves in inclined open channels," *Commun. Pure Appl. Math.*, **2**, 140–194 (1949).
2. G. B. Whitham, *Linear and Nonlinear Waves*, John Wiley and Sons, New York (1974).
3. H. Jeffreys, "The flow of water in an inclined channel of rectangular section," *Philos. Mag. Ser. 6*, **49**, 793–807 (1925).
4. V. M. Ponce and D. B. Simons, "Shallow wave propagation in open channel flow ," *J. Hydraul. Div.*, **103**, No. 12, 1461–1476 (1977).
5. R. R. Brock, "Development of roll-wave trains in open channels," *J. Hydraul. Div.*, **95**, No. HY4, 1401–1427 (1969).
6. D. J. Needham and J. H. Merkin, "On roll waves down an open inclined channel," *Proc. Roy. Soc. London, Ser. A*, **394**, 259–278 (1981).
7. C. Kranenburg, "On the evolution of roll waves," *J. Fluid Mech.*, **245**, 249–261 (1992).
8. J. Yu and J. Kevorkian, "Nonlinear evolution of small disturbances into roll waves in an inclined open channel," *J. Fluid Mech.*, **243**, 257–295 (1992).
9. S.-J. Lee, G. T. Yates, and T. Y. Vu, "Experiments and analyses of upstream-advancing solitary waves generated by moving disturbances," *J. Fluid Mech.*, **199**, 569–593 (1989).
10. F. Serre, "Contribution a l'etude des ecoulements permanents et variables dans les canaux," *La Houille Blanche*, Juin–Juill, 374–388 (1953).
11. V. Yu. Liapidevskii and V. M. Teshukov, *Mathematical Models of Long Wave Propagation in an Inhomogeneous Liquid* [in Russian], Izd. Sib. Otd. Ross. Akad. Nauk, Novosibirsk (2000).
12. V. Alavian, "Behavior of density currents on an incline," *J. Hydraul. Eng.*, **112**, No. 1, 27–42 (1986).